Horizontal gene transfer of a functional *cki* homolog in the human pathogen *Schistosoma mansoni*

George Wendt, James J. Collins III*

Department of Pharmacology, University of Texas Southwestern Medical Center

* To whom correspondence should be addressed

Abstract

Schistosomes are parasitic flatworms responsible for the neglected tropical disease schistosomiasis, causing devastating morbidity and mortality in the developing world. The parasites are protected by a skin-like tegument, and maintenance of this tegument is controlled by a schistosome ortholog of the tumor suppressor TP53. To understand mechanistically how *p53-1* controls tegument production, we identified a cyclin dependent kinase inhibitor homolog (*cki*) that was co-expressed with *p53-1*. RNA interference of *cki* resulted in a hyperproliferation phenotype, that, in combination with *p53-1* RNA interference yielded abundant tumor-like growths, indicating that *cki* and *p53-1* are bona fide tumor suppressors in *Schistosoma mansoni*. Interestingly, *cki* homologs are widely present throughout parasitic flatworms but evidently absent from their free-living ancestors, suggesting this cki homolog came from an ancient horizontal gene transfer event. This in turn implies that the evolution of parasitism in flatworms may have been aided by a highly unusual means of metazoan genetic inheritance.

Introduction

Parasitic flatworms are a diverse clade of organisms that include pathogens of great medical and agricultural purposes. Interestingly, all parasitic flatworms come from a single speciation event, and therefore are a derived clade relative to all free-living flatworms[1]. As such, common traits shared across parasitic flatworms could represent early adaptations that facilitated a free-living

ancestor in their transition to parasitic lifestyle. One such common trait is the presence of a tegument, a syncytial skin-like tissue that acts as the interface between the host and the parasite. The tegument is thought to be essential for parasitic flatworms, facilitating processes such as immune evasion, nutrient acquisition, and protection from physical and chemical insults[2-4].

The most medically important parasitic flatworms are the blood-dwelling parasites known as schistosomes. These parasites infect over 200 million of the world's poorest people, killing tens of thousands every year[5]. They reside in the vasculature of the host, where they can survive for decades, laying eggs that ultimately cause the pathology of schistosome infection[6]. The ability of the parasite to thrive within their host's bloodstream for decades on end is thought to be modulated by the parasite's stem cells and their tegument. Previous work has shown that in adult worms, stem cells are almost entirely dedicated to maintaining the schistosome's tegument[7, 8]. This tegument maintenance is regulated by a number of different factors including flatworm-specific transcription factors[8] and a parasite ortholog of *TP53* termed *Sman-p53-1* (henceforth *p53-1* for brevity, gene symbol Smp_139530)[9].

Despite being most widely recognized as a tumor suppressor, *TP53* homologs appear to play a different role in flatworms. Most free-living flatworms have a single *TP53* ortholog that is essential for the maintenance of a sub-population of their stem cells responsible for producing the worm's epidermis[10, 11]. Schistosomes have two TP53 homologs: a TP53 ortholog (*p53-1*) that is responsible for maintaining the stem cells responsible for producing the parasite's tegument and a second p53 molecule (*p53-2*, gene symbol Smp_136160) that is paralogous to *p53-1* that is only found in parasitic flatworms. Interestingly, the schistosome *p53-2* is required for the parasite's response to genotoxic stress[9]. Mechanistically, it is unclear how either of these TP53 homologs function.

One of the most well characterized mechanisms of TP53 function involves its regulation of the expression of the cyclin dependent kinase inhibitor (CKI) *P21/CDKN1A[12]*. In response to insults

49 such as genotoxic stress, TP53 induces the expression of P21. P21 then binds to and inhibits
50 cyclin dependent kinase (CDK)/cyclin complexes, resulting in the hypophosphorylation of RB,
51 preventing progression through the G1-S checkpoint[12, 13]. While direct regulation of CKIs by
52 P53 homologs is best characterized in vertebrates[14, 15], the interactions between CKIs, CDKs,
53 cyclins, and RB homologs seems to be broadly conserved across all metazoans[16, 17].

54 In this study, we attempted to understand how *p53-1* regulates tegument production in
55 schistosomes. In doing so, we identified a cyclin dependent kinase inhibitor that we termed *Sman-*
56 *cki* (henceforth *cki* for brevity, gene symbol Smp_199050). Functional studies of *cki* showed that
57 it is required for normal stem cell proliferation and differentiation. We also show that *cki* and *p53-*
58 *1* cooperate as tumor suppressors in *Schistosoma mansoni*. Interestingly, *cki* homologs were
59 present in almost every parasitic flatworm genome examined, but entirely absent from free-living
60 flatworms. Given the evolutionary relationship between free-living and parasitic flatworms, this
61 makes horizontal gene transfer (HGT) the likely origin of *cki* in parasitic flatworms.

62 **Results**

63 Having previously found that *p53-1*, the schistosome homolog of TP53, plays an important role in
64 tegument development[9], we sought to identify the targets of this transcription factor to
65 understand how *p53-1* controls tegument development. One common mechanism by which TP53
66 homologs function across different animals is by inducing the expression of cyclin dependent
67 kinase inhibitors such as *CDKN1A[15, 18]*. We identified a distant homolog of *CDKN1A* in the
68 *Schistosoma mansoni* genome (*Sman-cki*, henceforth *cki*) that was expressed in many of the
69 same cells as *p53-1*, including tegument progenitor cells and stem cells, suggesting it could play
70 a role in regulating tegument production (**Figure 1A-C**). Though this homolog did not possess an
71 annotated cyclin dependent kinase inhibitor (CDI) domain (InterPro entries
72 IPR044898/IPR003175[19]), it did bear high similarity and identity to other CDI-domain containing
73 proteins such as Drosophila Dap and human CDKN1B (**Figure S1A-C**). Additionally, the

74 AlphaFold[20] predicted structure of the n-terminus of CKI conformed to the structure of CDKN1B
75 when superimposed on the solved structure of CDK4/CCND1/CDKN1B[21] (**Figure S1C**).

76 We next tested the function of *cki* in the parasite. In other organisms, *cki* homologs act as tumor
77 suppressors in part by binding to and inhibiting the cyclin/cdk complexes that control the cell cycle,
78 halting proliferation[22]. As such, loss of function of *cki* homologs results in hyperproliferation in a
79 variety of animals in a variety of contexts[16, 17, 23-26]. When we knockdown *cki* using RNAi, we
80 similarly observe a hyperproliferation phenotype (**Figure 2, Figure S2A-B**). While there is nearly
81 100% penetrance of the hyperproliferation phenotype in the parasite's head (**Figure 2, top**), there
82 is variable penetrance of the phenotype in the body of the worm (**Figure 2, bottom**). This increase
83 in proliferation is also accompanied by a loss of production of *tsp-2*$^{+}$ tegument progenitor cells
84 (**Figure 2, Figure S2A-B**) as well as new tegument cells (**Figure S2C-D**), demonstrating that the
85 increase in proliferation is accompanied by a loss of differentiation. Additionally, we see an
86 approximately five-fold increase in apoptotic cells in the heads of *cki(RNAi)* parasites (**Figure**
87 **S2E-F]**). Together, this suggests that *cki* RNAi causes stem cells to engage in hyperproliferation
88 at the expense of differentiation, ultimately resulting in stem cell death.

89 Human *cki* homologs are widely recognized as tumor suppressors[22, 27], but no studies of
90 invertebrate *cki* homologs have demonstrated spontaneous tumor formation in *cki* loss-of-function
91 models[16, 23-25]. Unlike invertebrate models tested to date, schistosomes have lifespans
92 measured in decades[6] and rely upon proliferative somatic cells throughout these long lives[28].
93 As such, we wondered whether *cki* could function as a tumor suppressor in schistosomes.
94 Knockdown of *cki* alone causes hyperproliferation (**Figure 2**), but never results in robust
95 tumorigenesis. Given our original model that *cki* expression might be induced by *P53-1* (**Figure**
96 **3A**), we next wondered whether knocking down *p53-1* in combination with *cki* would create a
97 more permissive environment for tumor formation in the parasite. We found that knocking down
98 *p53-1* in conjunction with *cki* does in fact result in the appearance of abnormal proliferative tumor-

like masses in the parasite's head with nearly 100% penetrance (**Figure 3B**). This suggests that *cki* and *p53-1* cooperate as tumor suppressors in *Schistosoma mansoni* (**Figure 3C**).

Interestingly, we were able to readily identify *cki* homologs in nearly all parasitic flatworm genomes (present in 43 out of 47 examined) (**Table S1**) but were unable to find any *cki* homologs in any free-living flatworm genomes (present in 0 out of 19 genomes examined across 9 taxonomic orders) (**Figure 4A**). This is surprising because phylogenetic analysis suggests that all parasitic flatworms arose from a common free-living ancestor approximately 200 million years ago[1]. As such, any gene found broadly across parasitic clades should be present at some frequency in the extant free-living flatworms. The fact that we do not observe this suggests either 1) the parasite *cki* homologs arose from de novo gene birth, 2) *cki* homologs were present broadly throughout all flatworms but were independently lost in all extant free-living flatworm lineages that we have genomes for, or 3) the parasite *cki* homolog was not inherited "vertically" and therefore may have originated from horizontal gene transfer in an ancestral parasitic flatworm. Given that parasite *cki* homologs have sequence-level similarity to other metazoan *cki* homologs (**Figure S1A-B**), de novo gene birth can be ruled out. While we cannot rule out multiple independent losses of *cki* homologs across extant free-living flatworms, it would be incredibly unlikely that *cki* homologs were independently lost in 19 different animals across 9 taxonomic orders, leaving HGT as a plausible explanation for the origin of parasitic flatworm *cki*.

To search for evidence of a more typical (i.e., 'vertical') inheritance of *cki*, we decided to examine sequence changes across evolution in genes that are likely to have co-evolved with *cki*. In this case, we chose to examine cyclin dependent kinase 4 (*cdk4*) and cyclin d (*ccnd*) because they interact with each other and with *cki* homologs across diverse metazoans[17, 29]. They are also all present in the three groups of animals we chose to examine: parasitic flatworms, the relatively closely related molluscs, and the outgroup bony fish (**Figure 4A**). We reasoned that phylogenetic analysis of the sequences of 'vertically' inherited genes should recapitulate the phylogeny as we

124 know it to exist (that is to say, our bootstrap analysis should indicate that parasitic flatworm genes
125 are more similar to the closely related mollusc genes than they are to their bony fish counterparts).
126 This is indeed what we see when we analyze the sequences of CDK4 and CCND homologs, but
127 examination of CKI homologs is unable to robustly identify the correct phylogeny (**Figure 4B,**
128 **Figures S3-S7**). Combined with the phylogenetic relationship between free-living and parasitic
129 flatworms, this further supports HGT as the likely origin of *cki* in parasitic flatworms.

130 **Discussion**

131 Tumor suppressors such as TP53 and CDKN1A are some of the most widely studied molecules
132 on the planet, but their functions in animals that do not generally develop tumors are largely
133 unexplored. Here, we show that schistosomes have a *CDKN1A* homolog, *cki*, that acts as a tumor
134 suppressor together with the parasite's *TP53* ortholog, *p53-1*. Knocking down this *cki* homolog
135 results in a dramatic increase in stem cell proliferation with a concomitant decrease in
136 differentiation. Knocking down *cki* in combination with *p53-1* results in spontaneous and robust
137 formation of abnormal proliferative masses of cells, making *cki* and *p53-1* bona fide tumor
138 suppressors in schistosomes. Further studies of these tumors could better describe their
139 molecular identity and their cell of origin.

140 One exciting implication of this study is that schistosomes (and likely other parasitic flatworms)
141 possess a functional *cki* homolog, implying that cyclin-dependent kinases may be important in
142 regulating cellular proliferation in parasitic flatworms. One potential new area for schistosomacidal
143 drug development is the targeting of the parasite's stem cells. Previous studies have shown that
144 disrupting schistosome tissues maintained by stem cells is capable of injuring parasites[8] or
145 preventing disease pathology[30]. One of the greatest challenges in targeting parasite stem cells,
146 however, is identifying a way to specifically target proliferative cells in the parasite while sparing
147 proliferating cells in the host. Future work determining exactly which CDKs are involved in
148 regulating stem cells in schistosomes could reveal novel drug targets that could have good

149 therapeutic properties; CDK4/6 inhibitors, for example, are a relatively new family of anti-tumor
150 drugs that are generally well tolerated by patients[31, 32]. Schistosome CDK4 is relatively
151 divergent compared to human CDK4. The schistosome CDK4 kinase domain has 41.2%/63.9%
152 identity/similarity to human CDK4, comparable to the difference between human CDK4 and
153 human CDK1 (43.4%/62.0%), and CDK4 inhibitors are generally very specific (the CDK4/6
154 inhibitor Palbociclib has >1000 fold selectivity for CDK4 over CDK1[33]), suggesting that
155 schistosome CDK4 has potential to be a selective drug target. Further studies of *cki* and its
156 interacting molecules could therefore have significant therapeutic implications for combatting
157 schistosomiasis.

158 Perhaps most interestingly, one of the most likely origins of the parasite's *cki* homolog is horizontal
159 gene transfer. Given that parasitic flatworms all derive from a common free-living ancestor[1],
160 anything ubiquitous in parasitic flatworms should be present at some frequency in extant free-
161 living flatworms. That *cki* is absent from free-living flatworms led us to 3 very unlikely explanations
162 for its origin. First, we believe we can safely rule out de novo gene birth given that parasite *cki* is
163 related to other metazoan *cki* homologs on the sequence level (**Figure S1A-B**). That leaves us
164 with either 1) a situation where *cki* homologs were broadly present throughout all flatworms, but
165 then sometime after parasitic flatworms diverged 200 million years ago, the ancestors of all extant
166 free-living flatworm lineages lost their *cki* homologs while parasitic flatworms retained theirs or 2)
167 a situation where an early ancestral parasitic flatworm acquired a *cki* homolog via horizontal gene
168 transfer. Definitive proof of horizontal gene transfer would require us to be able to identify the non-
169 flatworm animal that has a *cki* homolog with sequence similarity to the flatworm molecule.
170 Unfortunately, we have been unable to find such an animal, possibly because this animal would
171 have had to been alive approximately 200 million years ago (in order to transmit its *cki* homolog
172 to the ancestral parasitic flatworm) and may not have survived to create modern descendants. As

173 such, rather than stating that parasitic flatworm *cki* came from horizontal gene transfer, we instead
174 propose that horizontal gene transfer is one of the most plausible origins for this *cki*.

175 Further complicating the assumption that parasite *cki* came from horizontal gene transfer, HGT in
176 metazoans, especially between metazoans, is relatively rare[34, 35]. Still, HGT in parasitic
177 flatworms might be more common than in other metazoans. HGT between multicellular organisms
178 has been frequently identified between parasitic plants and their host plants[36-39]. Aside from
179 the analogous relationship between parasitic flatworms and their metazoan hosts, parasitic
180 flatworms may represent especially molecularly fertile ground for HGT. In addition to their syncytial
181 tegument, all parasitic flatworms are also united by their loss of the piRNA pathway[40] that,
182 combined with apparent the lack of DNA methylation across flatworms[41-43], makes the parasitic
183 flatworms deficient in two key pathways used to suppress mobile selfish genetic elements like
184 transposons and endogenous retroviruses[34, 44, 45]. Indeed, this type of HGT has been
185 reported between parasitic lamprey and their host[46], both of which have intact defenses against
186 selfish genetic elements. Selfish genetic element mediated HGT could therefore be unusually
187 successful in parasitic flatworms.

188 Origin of *cki* gene notwithstanding, the fact that it is nearly ubiquitous across all parasitic flatworms
189 means that it has been present in parasitic flatworms from early in their evolution and has likely
190 been retained because it plays an important role in these animals. Understanding that role could
191 teach us not only about the evolution of parasitism in these fascinating animals but could also
192 reveal ways to combat the diseases that they cause.

193 **Figure Legends**

194 Figure 1. Expression pattern of *cki*. A) Uniform manifold approximation plots showing expression
195 patterns of *p53-1* and *cki* in adult schistosomes. Red indicates high expression, orange indicates
196 medium expression, and blue indicates low/no expression. B) Colorimetric WISH showing

197 expression patterns of *cki* in male (left) and female (right) worms. H, head; T, testes; O, ovary; V,
198 vitellaria. C) Double FISH experiment showing expression of *cki* relative to the tegument
199 progenitor marker *tsp-2*, the proliferative cell marker *h2b*, and *p53-1*. Scale bars: (B) 500 μm, (C)
200 5 μm.

201 Figure 2. *cki* RNAi results in an increase in proliferation at the expense of differentiation. FISH
202 experiment in conjunction with EdU detection showing expression pattern of the tegument
203 progenitor marker *tsp-2* (green) in conjunction with the presence of proliferative EdU^+ cells
204 (yellow) under the indicated RNAi conditions. The fraction indicates the number of worms that are
205 similar to the representative image. Data are from 3 biological replicates. Scale bar: 50 μm.

206 Figure 3. *cki* and *p53-1* cooperate as tumor suppressors in *Schistosoma mansoni*. (A) Cartoon
207 depicting model of *p53-1* and *cki* interaction in normal parasites. In proliferative cells, P53-1
208 activity is low and *cki* is not transcribed, resulting in active cyclin/CDK complexes, promoting
209 proliferation. When proliferative cells commit to differentiating, P53-1 activity is high and *cki* is
210 transcribed, resulting in inactive cyclin/CDK/CKI complexes, promoting differentiation. (B) EdU
211 labelled neoblasts in parasites treated witih control RNAi, *p53-1* RNAi, *cki* RNAi, or a combination
212 of *p53-1* and *cki* RNAi. (C) Cartoon depicting consequences of *cki* RNAi. By knocking down *cki*,
213 cyclin/CDK complexes are inappropriately active, leading to increased proliferation and
214 decreased differentiation. (D) Cartoon depicting consequences of knocking down *cki* and *p53-1*
215 simultaneously. Knocking down *cki* directly depletes CKI protein. Knocking down *p53-1* decreases
216 P53-1-dependent induction of *cki* expression. This combination may lower CKI levels low enough
217 that proliferating cells become abnormal and form tumors. The fraction indicates the number of
218 worms that are similar to the representative image. Scale bar: 50 μm.

219 Figure 4. Phylogeny of CKI. (A) Top. Cladogram of *cki* homologs across select metazoans.
220 Bottom. Chart indicating the presence or absence of *cdk4*, *ccnd*, and *cki* homologs in the above
221 species. Green circles indicate presence and red x's indicate absence. (B) Simplification of

222 phylogenetic analysis of aligned sequences of CDK4, CCND, and CKI homologs across bony
223 fish, molluscs, and parasitic flatworms. Circle with the number indicates the bootstrap value of the
224 bifurcation between molluscs and parasitic flatworms. The color of the circle indicates relative
225 confidence of tree structure, where green is high and red is low.

226 Figure S1. Sman-CKI protein domains/structure. (A) Clustal alignment of CKI sequences from a
227 variety of parasitic flatworms as well as human CDKN1B. Dashed lines indicate parts of
228 alignments that fall within a CDI domain (InterPro IPR044898). The number at top of alignment
229 corresponds to position in the alignment relative to the *Schistosoma mansoni* CKI. Protein
230 sequences used for alignment and species abbreviations can be found in **Table S2** (B) Schematic
231 of the domain structure of CKI homologs from *S. mansoni*, *E. granulosus*, *D. melanogaster*, and
232 *H. sapiens* along with the percentage identity/similarity relative to the *S. mansoni* CKI homolog.
233 (C) Superimposition of the AlphaFold indicated residues of *S. mansoni* CKI (accession:
234 AF_A0A3Q0KUT0-F1-model_v4) onto the solved structure of *H. sapiens* CDKN1B, CCND1, and
235 CDK4 (PDB accession: 6p8e). Hash-shaded portion from (B) corresponds to the superimposition
236 in (C).

237 Figure S2. *cki* RNAi results in an increase in proliferation at the expense of differentiation. (A)
238 qPCR showing expression of *cki*, the stem cell marker *nanos2*, and the tegument progenitor
239 marker *tsp-2* under indicated RNAi conditions. 'cki(RNAi)(alt)' indicates knockdown performed
240 with dsRNA corresponding to a non-overlapping sequence relative to the original dsRNA
241 sequence. (B) FISH experiment in conjunction with EdU detection showing expression pattern of
242 the tegument progenitor marker *tsp-2* (green) in conjunction with the presence of proliferative
243 EdU^+ cells (yellow) under the indicated RNAi conditions. Note that the micrographs for
244 control(RNAi) are duplicates of the micrographs for control(RNAi) from Figure 3 (top) as these
245 came from the same experiment. (C) FISH of the tegument marker *calp* after control or *cki* RNAi.
246 Neoblast progeny are labeled with the EdU via a pulse-chase experiment. (D) Quantification of

247 (C). (E) Fluorescent TUNEL assay labeling DNA breaks in worms under the indicated RNAi
248 conditions. T, testes. Scale bar: 50 μm. Note signal in the testes is a normal occurrence in the
249 parasite's proliferative germline. (F) Quantification of (E). Scale bars: (B) 50 μm, (C) 10 μm. (E)
250 50 μm.

251 Figure S3. Phylogeny of CDK4 excluding free-living flatworms. Phylogenetic tree based on
252 analysis of aligned protein sequences of CDK4 homologs across a sampling of bony fish,
253 molluscs, and parasitic flatworms. The bifurcation point of molluscs and parasitic flatworms is
254 indicated with a circle. The tree is arbitrarily rooted to *D. rerio*. Species name abbreviations and
255 protein sequences are available in **Table S3**. Numbers indicate bootstrap values. Scale bar: 1
256 substitution/site.

257 Figure S4. Phylogeny of CDK4 including free-living flatworms. Phylogenetic tree based on
258 analysis of aligned protein sequences of CDK4 homologs across a sampling of bony fish,
259 molluscs, free-living, and parasitic flatworms. Numbers indicate bootstrap values. The tree is
260 arbitrarily rooted to *D. rerio*. Species name abbreviations and protein sequences are available in
261 **Table S4**. Numbers indicate bootstrap values. Scale bar: 1 substitution/site.

262 Figure S5. Phylogeny of CCND excluding free-living flatworms. Phylogenetic tree based on
263 analysis of aligned protein sequences of CCND homologs across a sampling of bony fish,
264 molluscs, and parasitic flatworms. The bifurcation point of molluscs and parasitic flatworms is
265 indicated with a circle. Numbers indicate bootstrap values. The tree is arbitrarily rooted to *D. rerio*.
266 Species name abbreviations and protein sequences are available in **Table S5**. Numbers indicate
267 bootstrap values. Scale bar: 1 substitution/site.

268 Figure S6. Phylogeny of CCND including free-living flatworms. Phylogenetic tree based on
269 analysis of aligned protein sequences of CCND homologs across a sampling of bony fish,
270 molluscs, and parasitic flatworms. The bifurcation point of molluscs and parasitic flatworms is

271 indicated with a circle. Numbers indicate bootstrap values. The tree is arbitrarily rooted to *D. rerio*.
272 Species name abbreviations and protein sequences are available in **Table S6**. Numbers indicate
273 bootstrap values. Scale bar: 1 substitution/site.

274 Figure S7. Phylogeny of CKI. Phylogenetic tree based on analysis of aligned protein sequences
275 of CKI homologs across a sampling of bony fish, molluscs, and parasitic flatworms. The bifurcation
276 point of molluscs and parasitic flatworms is indicated with a circle. Numbers indicate bootstrap
277 values. The tree is arbitrarily rooted to *D. rerio*. Species name abbreviations and protein
278 sequences are available in **Table S7**. Numbers indicate bootstrap values. Scale bar: 1
279 substitution/site.

280 **Materials and Methods**

281 *Phylogenetic analysis*

282 Identification of orthologs of *Schistosoma mansoni cki* homologs was carried out using Wormbase
283 Parasite (https://parasite.wormbase.org/)(version 19.0 (March 2024))[47, 48]. Examination of
284 *Sman-cki* (Smp_199050) homologs initially only revealed *cki* homologs in trematodes (present in
285 27/28 unique genomes) and monogeneans (present in 1/3 unique genomes). A reciprocal BLAST
286 search of the *Hymenolepis diminuta* genome identified the *cki* homolog WMSIL1_LOCUS6166
287 ("CDI domain-containing protein"). Wormbase Parasite then identified 12 orthologs of
288 WMSIL1_LOCUS6166 in 11 unique cestode genomes, each of which was confirmed to be a *cki*
289 ortholog via a reciprocal BLAST search. Additional BLAST searches of cestode genomes
290 revealed 4 additional *cki* homologs in cestodes (in total present in 15/16 unique genomes), with
291 two being incorrectly included in the gene model of TIMM21 homologs (see **Table S2**). PlanMine
292 v3.0 (https://planmine.mpinat.mpg.de/planmine/)[49] was utilized in order to search 19 free-living
293 flatworm genomes for *cki* homologs. Domain structure of CKI homologs was obtained using
294 SMART v9.0 (http://smart.embl-heidelberg.de/)[50, 51].

295 Clustal alignment of CKI sequences was performed using Clustal Omega Multiple Sequence
296 Alignment[52] with default settings except ORDER was set to 'input'[53, 54]. Protein sequences
297 used for alignment and species abbreviations can be found in **Table S2**.

298 Phylogenetic trees were generated from CKI protein sequences by first using Clustal Omega[52]
299 to perform multiple sequence alignments using default settings. Aligned sequences were then
300 analyzed using RAxML (Version 8.2.12[55, 56]]) via raxmlGUI (version 2.0.10[57]) with the
301 following parameters:

302 -T 10 -f a -x 756002 -p 756002 -N 1000 -m PROTGAMMAJTTF -k -O (for analysis of CKI
303 homologs),

304 -T 10 -f a -x 756002 -p 756002 -N 1000 -m PROTGAMMAIJTTF -k -O (for analysis of CDK4
305 homologs both including and excluding free-living flatworms)

306 -T 10 -f a -x 296744 -p 296744 -N 1000 -m PROTGAMMAIJTTF -k -O (for analysis of CCND
307 homologs including free-living flatworms)

308 -T 10 -f a -x 756002 -p 756002 -N 1000 -m PROTGAMMAIJTTF -k -O (for analysis of CCND
309 homologs excluding free living flatworms)

310 The best model was determined using ModelTest-NG (version 0.1.7[58]). The best maximum-
311 likelihood tree was visualized using Interactive Tree of Life[59] and rooted to *Danio rerio* for visual
312 consistency.

313 All sequences used for phylogenetic analysis are available in **Tables S3-S7**.

314 *Parasite acquisition and culture*

315 Adult S. mansoni (NMRI strain, 6–7 weeks post-infection) were obtained from infected female
316 mice by hepatic portal vein perfusion with 37°C DMEM (Sigma-Aldrich, St. Louis, MO) plus 10%
317 Serum (either Fetal Calf Serum or Horse Serum) and heparin. Parasites were cultured as

318 previously described[7]. Unless otherwise noted, all experiments were performed with male
319 parasites in order to maximize the amount of somatic tissue present and to avoid additional
320 experimental modifications that have to be undertaken for successful in vitro female parasite
321 culture[60]. Experiments with and care of vertebrate animals were performed in accordance with
322 protocols approved by the Institutional Animal Care and Use Committee (IACUC) of UT
323 Southwestern Medical Center (approval APN: 2017-102092).

324 *Labeling and imaging*

325 Schistosome colorimetric and fluorescence in situ hybridization analyses were performed as
326 previously described[7-9, 28] with the following modification. To improve signal-to-noise for
327 colorimetric and fluorescence in situ hybridization, worms were incubated at 95°C for 15m in
328 10mM sodium citrate, pH6.0 prior to proteinase K digestion. *in vitro* EdU labeling and detection
329 was performed as previously described[61]. TUNEL labeling was carried out as follows:
330 formaldehyde-fixed worms stored in 100% MeOH were rehydrated in 50% MeOH/50% PBS +
331 0.3% TritonX-100 pH7.4 (PBSTx), then rinsed in PBSTx. Parasites were then photobleached as
332 described previously[7]. After photobleaching, parasites were rinsed in PBSTx, then incubated at
333 95°C for 15m in 10mM sodium citrate pH6.0. Following this, parasites were rinsed in PBSTx then
334 permeablized in 5 µg/ml proteinase K (Ambion AM2546). Following proteinase K treatment,
335 parasites were post-fixed in 4% formaldehyde in PBSTx. Parasites were then rinsed in PBSTx
336 then incubated at 37°C in TdT reaction buffer from Click-iT™ Plus TUNEL Assay for In Situ
337 Apoptosis Detection kit (Thermo Fisher Scientific C10617) for one hour. Parasites were then
338 incubated at 37°C in TdT reaction mix for one hour per manufacturer's instructions. Parasites
339 were then thoroughly rinsed and EdU detection was carried out as previously described[7]. All
340 fluorescently labeled parasites were counterstained with DAPI (1 µg/ml), cleared in 80% glycerol,
341 and mounted on slides with Vectashield (Vector Laboratories).

342 Confocal imaging of fluorescently labeled samples was performed on a Zeiss LSM900 Laser
343 Scanning Confocal Microscope. Unless otherwise mentioned, all fluorescence images represent
344 maximum intensity projection plots. To perform cell counts, cells were manually counted in
345 maximum intensity projection plots derived from confocal stacks. Brightfield images were acquired
346 on a Zeiss AxioZoom V16 equipped with a transmitted light base and a Zeiss AxioCam 105 Color
347 camera.

348 *RNA interference*

349 Schistosome RNAi: All RNAi experiments utilized freshly perfused male parasites between 6-7
350 weeks post-infection (separated from females). dsRNA treatments were all carried out at 30 µg/ml
351 in Basch Media 169. Double knockdown experiments were carried out at 60 µg/ml (30 µg/ml of
352 each dsRNA) for the first 4 days, then switched to 30 µg/ml (15 µg/ml of each dsRNA) for the
353 remainder of the experiment. dsRNA was generated by in vitro transcription and was replaced
354 daily for 3 days and then every other day until the end of the experiment (14 days for all
355 experiments except for EdU pulse-chase experiments, which were EdU pulsed at day 14 then
356 carried out for 8 more days). EdU pulses were performed at 5µM for 4 hours before either fixation
357 or chase as previously described.

358 As a negative control for RNAi experiments, we used a non-specific dsRNA containing two
359 bacterial genes(48). cDNAs used for RNAi and in situ hybridization analyses were cloned as
360 previously described(48); oligonucleotide primer sequences are listed in **Table S8**.

361 *Statistical analysis*

362 Statistical analysis was carried out using one-way ANOVA tests (qPCR experiments) or two-way
363 ANOVA with Tukey's multiple comparisons tests (all other experiments). All statistical tests were
364 performed using GraphPad Prism v10.2.3.

365 *Acknowledgments*

366 Schistosome infected mice and *B. glabrata* snails were provided by the National Institute of Allergy
367 and Infectious Diseases Schistosomiasis Resource Center of the Biomedical Research Institute
368 (Rockville, MD, USA) through National Institutes of Health National Institute of Allergy and
369 Infectious Diseases Contract HHSN272201700014I for distribution through BEI Resources.
370 Funding: This work was supported by the National Institutes of Health R01AI121037 (J.J.C.) and
371 R01AI150776(J.J.C.), as well as the Welch Foundation I-1948-20180324 (J.J.C.).

372 **References**

373 1. Laumer, C.E., A. Hejnol, and G. Giribet, *Nuclear genomic signals of the 'microturbellarian'*
374 *roots of platyhelminth evolutionary innovation*. Elife, 2015. **4**.
375 2. Alan Wilson, R. and M.K. Jones, *Fifty years of the schistosome tegument: discoveries,*
376 *controversies, and outstanding questions*. Int J Parasitol, 2021.
377 3. Fairweather, I., L.T. Threadgold, and R.E. Hanna, *Development of Fasciola hepatica in the*
378 *mammalian host*. Fasciolosis, 1999. **1**: p. 47-111.
379 4. Brehm, K. and U. Koziol, *Echinococcus-Host Interactions at Cellular and Molecular Levels*.
380 Adv Parasitol, 2017. **95**: p. 147-212.
381 5. Colley, D.G., et al., *Human schistosomiasis*. Lancet, 2014. **383**(9936): p. 2253-64.
382 6. Basch, P.F., *Schistosomes: Development, Reproduction, and Host Relations*. 1991, New
383 York: Oxford University Press. 248.
384 7. Collins, J.J., III, et al., *Stem cell progeny contribute to the schistosome host-parasite*
385 *interface*. Elife, 2016. **5**.
386 8. Wendt, G.R., et al., *Flatworm-specific transcriptional regulators promote the specification of*
387 *tegumental progenitors in Schistosoma mansoni*. Elife, 2018. **7**.
388 9. Wendt, G.R., et al., *Convergent evolution of a genotoxic stress response in a parasite-specific*
389 *p53 homolog*. Proc Natl Acad Sci U S A, 2022. **119**(37): p. e2205201119.
390 10. Cheng, L.C., et al., *Cellular, ultrastructural and molecular analyses of epidermal cell*
391 *development in the planarian Schmidtea mediterranea*. Dev Biol, 2018. **433**(2): p. 357-373.
392 11. Pearson, B.J. and A. Sánchez Alvarado, *A planarian p53 homolog regulates proliferation and*
393 *self-renewal in adult stem cell lineages*. Development, 2010. **137**(2): p. 213-21.
394 12. Engeland, K., *Cell cycle regulation: p53-p21-RB signaling*. Cell Death Differ, 2022. **29**(5): p.
395 946-960.
396 13. Harper, J.W., et al., *The p21 Cdk-interacting protein Cip1 is a potent inhibitor of G1 cyclin-*
397 *dependent kinases*. Cell, 1993. **75**(4): p. 805-16.
398 14. Berghmans, S., et al., *tp53 mutant zebrafish develop malignant peripheral nerve sheath*
399 *tumors*. Proc Natl Acad Sci U S A, 2005. **102**(2): p. 407-12.
400 15. el-Deiry, W.S., et al., *WAF1/CIP1 is induced in p53-mediated G1 arrest and apoptosis*. Cancer
401 Res, 1994. **54**(5): p. 1169-74.
402 16. de Nooij, J.C., M.A. Letendre, and I.K. Hariharan, *A cyclin-dependent kinase inhibitor,*
403 *Dacapo, is necessary for timely exit from the cell cycle during Drosophila embryogenesis*.
404 Cell, 1996. **87**(7): p. 1237-47.

17. Boxem, M. and S. van den Heuvel, *lin-35 Rb and cki-1 Cip/Kip cooperate in developmental regulation of G1 progression in C. elegans*. Development, 2001. **128**(21): p. 4349-59.
18. Langheinrich, U., et al., *Zebrafish as a model organism for the identification and characterization of drugs and genes affecting p53 signaling*. Curr Biol, 2002. **12**(23): p. 2023-8.
19. Paysan-Lafosse, T., et al., *InterPro in 2022*. Nucleic Acids Research, 2022. **51**(D1): p. D418-D427.
20. Varadi, M., et al., *AlphaFold Protein Structure Database in 2024: providing structure coverage for over 214 million protein sequences*. Nucleic Acids Research, 2023. **52**(D1): p. D368-D375.
21. Guiley, K.Z., et al., *p27 allosterically activates cyclin-dependent kinase 4 and antagonizes palbociclib inhibition*. Science, 2019. **366**(6471).
22. Csergeová, L., D. Krbušek, and R. Janoštiak, *CIP/KIP and INK4 families as hostages of oncogenic signaling*. Cell Div, 2024. **19**(1): p. 11.
23. Buck, S.H., D. Chiu, and R.M. Saito, *The cyclin-dependent kinase inhibitors, cki-1 and cki-2, act in overlapping but distinct pathways to control cell cycle quiescence during C. elegans development*. Cell Cycle, 2009. **8**(16): p. 2613-20.
24. Fukuyama, M., et al., *Essential embryonic roles of the CKI-1 cyclin-dependent kinase inhibitor in cell-cycle exit and morphogenesis in C elegans*. Dev Biol, 2003. **260**(1): p. 273-86.
25. Lane, M.E., et al., *Dacapo, a cyclin-dependent kinase inhibitor, stops cell proliferation during Drosophila development*. Cell, 1996. **87**(7): p. 1225-35.
26. Deng, C., et al., *Mice lacking p21CIP1/WAF1 undergo normal development, but are defective in G1 checkpoint control*. Cell, 1995. **82**(4): p. 675-84.
27. Abukhdeir, A.M. and B.H. Park, *P21 and p27: roles in carcinogenesis and drug resistance*. Expert Rev Mol Med, 2008. **10**: p. e19.
28. Collins, J.J., III, et al., *Adult somatic stem cells in the human parasite Schistosoma mansoni*. Nature, 2013. **494**(7438): p. 476-9.
29. Baker, S.J., et al., *CDK4: a master regulator of the cell cycle and its role in cancer*. Genes Cancer, 2022. **13**: p. 21-45.
30. Wendt, G., et al., *A single-cell RNA-seq atlas of Schistosoma mansoni identifies a key regulator of blood feeding*. Science, 2020. **369**(6511): p. 1644-1649.
31. Gharbi, S.I., et al., *Crystal structure of active CDK4-cyclin D and mechanistic basis for abemaciclib efficacy*. NPJ Breast Cancer, 2022. **8**(1): p. 126.
32. Gharbi, S.I., et al., *Author Correction: Crystal structure of active CDK4-cyclin D and mechanistic basis for abemaciclib efficacy*. NPJ Breast Cancer, 2022. **8**(1): p. 133.
33. Fry, D.W., et al., *Specific inhibition of cyclin-dependent kinase 4/6 by PD 0332991 and associated antitumor activity in human tumor xenografts*. Mol Cancer Ther, 2004. **3**(11): p. 1427-38.
34. Soucy, S.M., J. Huang, and J.P. Gogarten, *Horizontal gene transfer: building the web of life*. Nat Rev Genet, 2015. **16**(8): p. 472-82.
35. Pandey, T., et al., *Acquired stress resilience through bacteria-to-nematode interdomain horizontal gene transfer*. Embo j, 2023. **42**(24): p. e114835.
36. Yoshida, S., et al., *Horizontal gene transfer by the parasitic plant Striga hermonthica*. Science, 2010. **328**(5982): p. 1128.
37. Xi, Z., et al., *Horizontal transfer of expressed genes in a parasitic flowering plant*. BMC Genomics, 2012. **13**: p. 227.
38. Zhang, Y., et al., *Evolution of a horizontally acquired legume gene, albumin 1, in the parasitic plant Phelipanche aegyptiaca and related species*. BMC Evol Biol, 2013. **13**: p. 48.

452 39. Zhang, D., et al., *Root parasitic plant Orobanche aegyptiaca and shoot parasitic plant*
453 *Cuscuta australis obtained Brassicaceae-specific strictosidine synthase-like genes by*
454 *horizontal gene transfer*. BMC Plant Biol, 2014. **14**: p. 19.
455 40. Tsai, I.J., et al., *The genomes of four tapeworm species reveal adaptations to parasitism*.
456 Nature, 2013. **496**(7443): p. 57-63.
457 41. Raddatz, G., et al., *Dnmt2-dependent methylomes lack defined DNA methylation patterns*.
458 Proc Natl Acad Sci U S A, 2013. **110**(21): p. 8627-31.
459 42. Cox, G.S., C.K. Phares, and R.A. Schmidt, *Molecular characterization of the Spirometra*
460 *mansonoides genome: renaturation kinetics, methylation, and hybridization to human cDNA*
461 *probes*. Biochim Biophys Acta, 1990. **1049**(2): p. 134-44.
462 43. Fantappié, M.R., E.R. Gimba, and F.D. Rumjanek, *Lack of DNA methylation in Schistosoma*
463 *mansoni*. Exp Parasitol, 2001. **98**(3): p. 162-6.
464 44. Li, D., D.H. Taylor, and J.C. van Wolfswinkel, *PIWI-mediated control of tissue-specific*
465 *transposons is essential for somatic cell differentiation*. Cell Rep, 2021. **37**(1): p. 109776.
466 45. Goodier, J.L., *Restricting retrotransposons: a review*. Mob DNA, 2016. **7**: p. 16.
467 46. Zhang, H.H., et al., *Recurrent horizontal transfers of Chapaev transposons in diverse*
468 *invertebrate and vertebrate animals*. Genome Biol Evol, 2014. **6**(6): p. 1375-86.
469 47. Howe, K.L., et al., *WormBase ParaSite - a comprehensive resource for helminth genomics*.
470 Mol Biochem Parasitol, 2017. **215**: p. 2-10.
471 48. Howe, K.L., et al., *WormBase 2016: expanding to enable helminth genomic research*. Nucleic
472 Acids Res, 2016. **44**(D1): p. D774-80.
473 49. Rozanski, A., et al., *PlanMine 3.0-improvements to a mineable resource of flatworm biology*
474 *and biodiversity*. Nucleic Acids Res, 2019. **47**(D1): p. D812-d820.
475 50. Letunic, I. and P. Bork, *20 years of the SMART protein domain annotation resource*. Nucleic
476 Acids Research, 2017. **46**(D1): p. D493-D496.
477 51. Letunic, I., S. Khedkar, and P. Bork, *SMART: recent updates, new developments and status in*
478 *2020*. Nucleic Acids Res, 2021. **49**(D1): p. D458-d460.
479 52. Madeira, F., et al., *Search and sequence analysis tools services from EMBL-EBI in 2022*.
480 Nucleic acids research, 2022. **50**(W1): p. W276-W279.
481 53. Yachdav, G., et al., *MSAViewer: interactive JavaScript visualization of multiple sequence*
482 *alignments*. Bioinformatics, 2016. **32**(22): p. 3501-3503.
483 54. Lemoine, F., et al., *NGPhylogeny.fr: new generation phylogenetic services for non-specialists*.
484 Nucleic Acids Res, 2019. **47**(W1): p. W260-w265.
485 55. Stamatakis, A., *RAxML version 8: a tool for phylogenetic analysis and post-analysis of large*
486 *phylogenies*. Bioinformatics, 2014. **30**(9): p. 1312-3.
487 56. Kozlov, A.M., et al., *RAxML-NG: a fast, scalable and user-friendly tool for maximum likelihood*
488 *phylogenetic inference*. Bioinformatics, 2019. **35**(21): p. 4453-4455.
489 57. Edler, D., et al., *raxmlGUI 2.0: A graphical interface and toolkit for phylogenetic analyses using*
490 *RAxML*. Methods in Ecology and Evolution, 2021. **12**(2): p. 373-377.
491 58. Darriba, D., et al., *ModelTest-NG: A New and Scalable Tool for the Selection of DNA and*
492 *Protein Evolutionary Models*. Mol Biol Evol, 2020. **37**(1): p. 291-294.
493 59. Letunic, I. and P. Bork, *Interactive Tree of Life (iTOL) v6: recent updates to the phylogenetic*
494 *tree display and annotation tool*. Nucleic Acids Research, 2024.
495 60. Wang, J., R. Chen, and J.J. Collins, III, *Systematically improved in vitro culture conditions*
496 *reveal new insights into the reproductive biology of the human parasite Schistosoma*
497 *mansoni*. PLoS Biol, 2019. **17**(5): p. e3000254.
498 61. Collins, J.J., III and P.A. Newmark, *It's no fluke: the planarian as a model for understanding*
499 *schistosomes*. PLoS Pathog, 2013. **9**(7): p. e1003396.

500

501

Figure 1: Expression

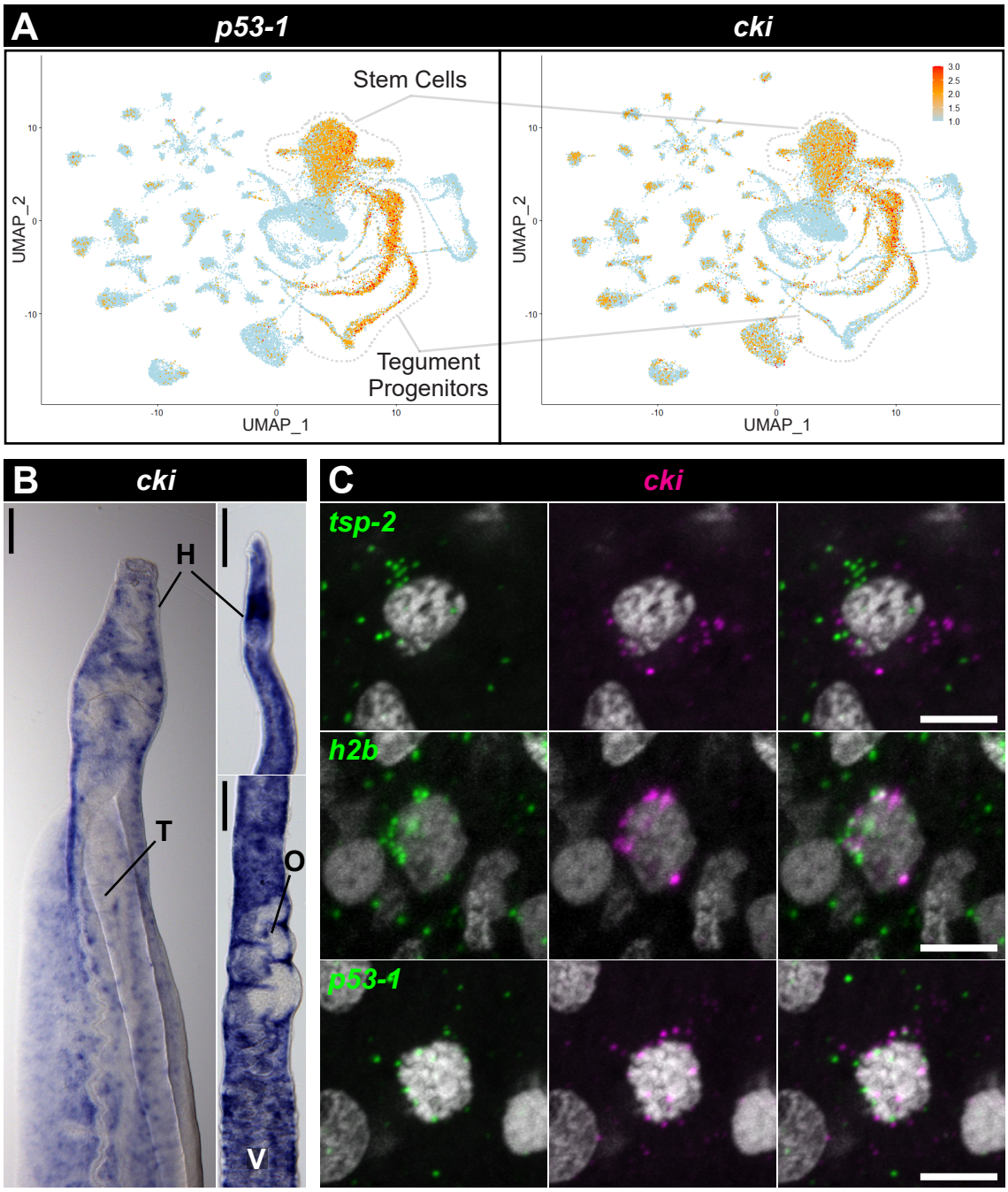

Figure S1: Protein Domains/Structure

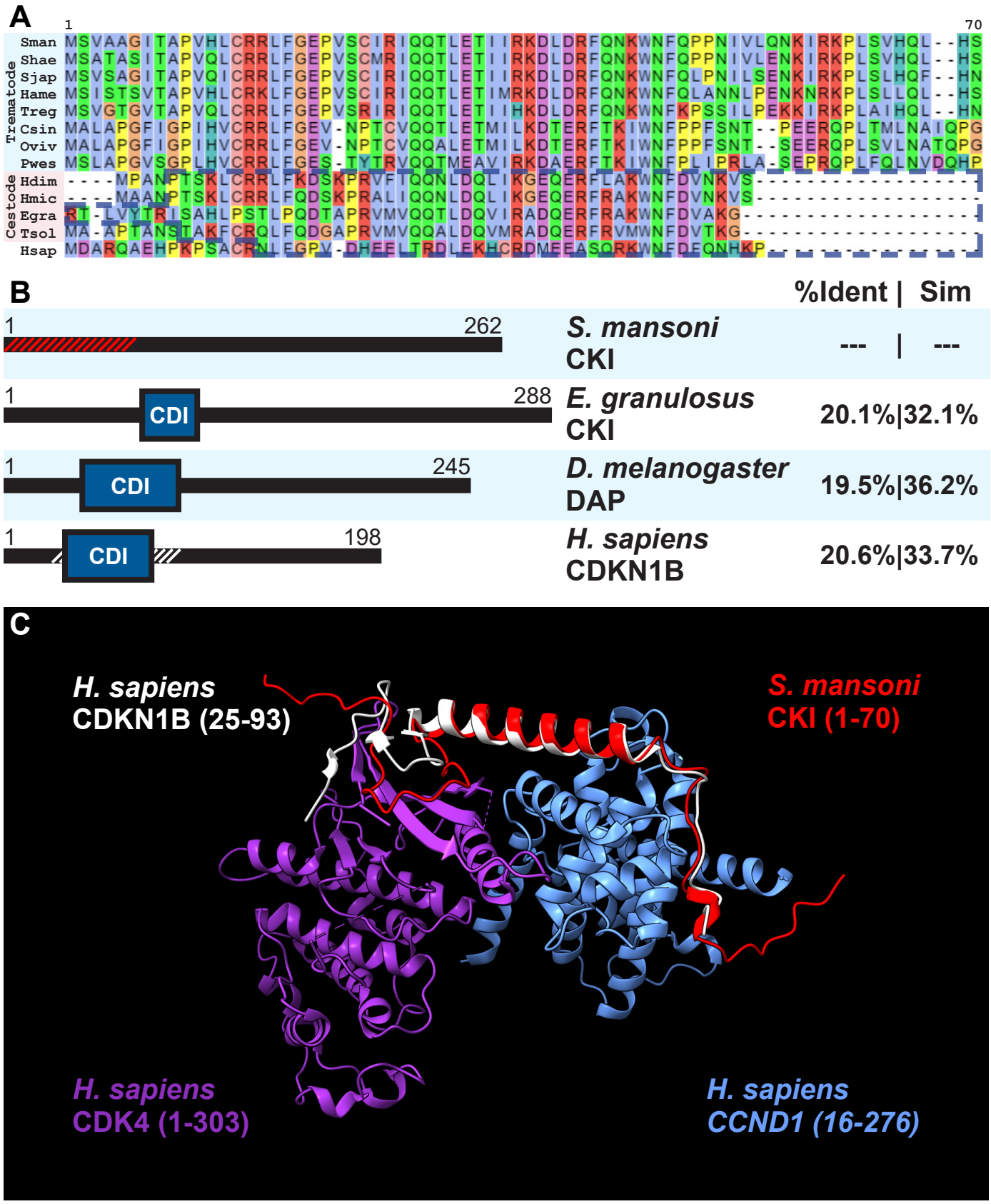

Figure 2: RNAi

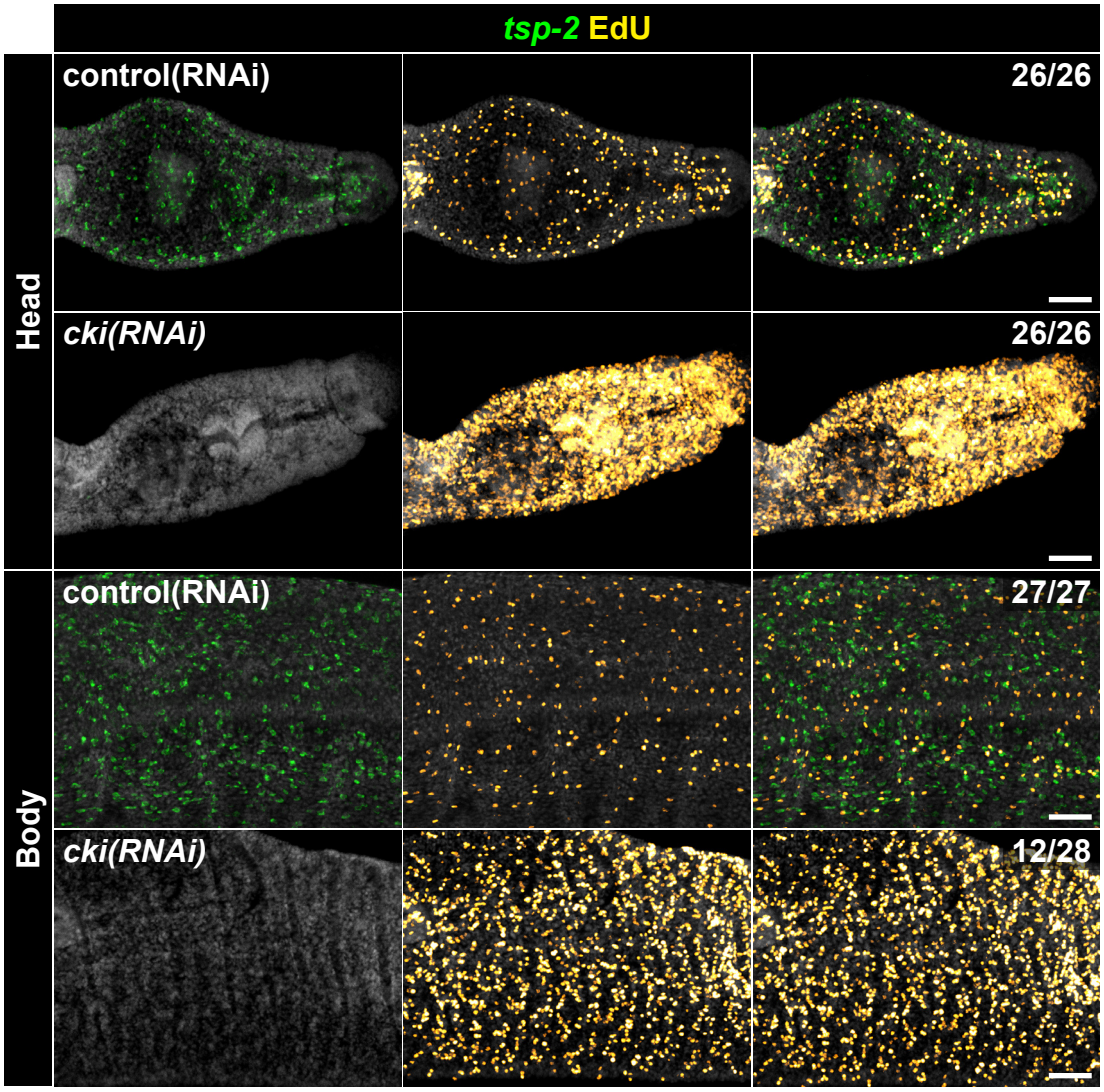

Figure S2 RNAi phenotype

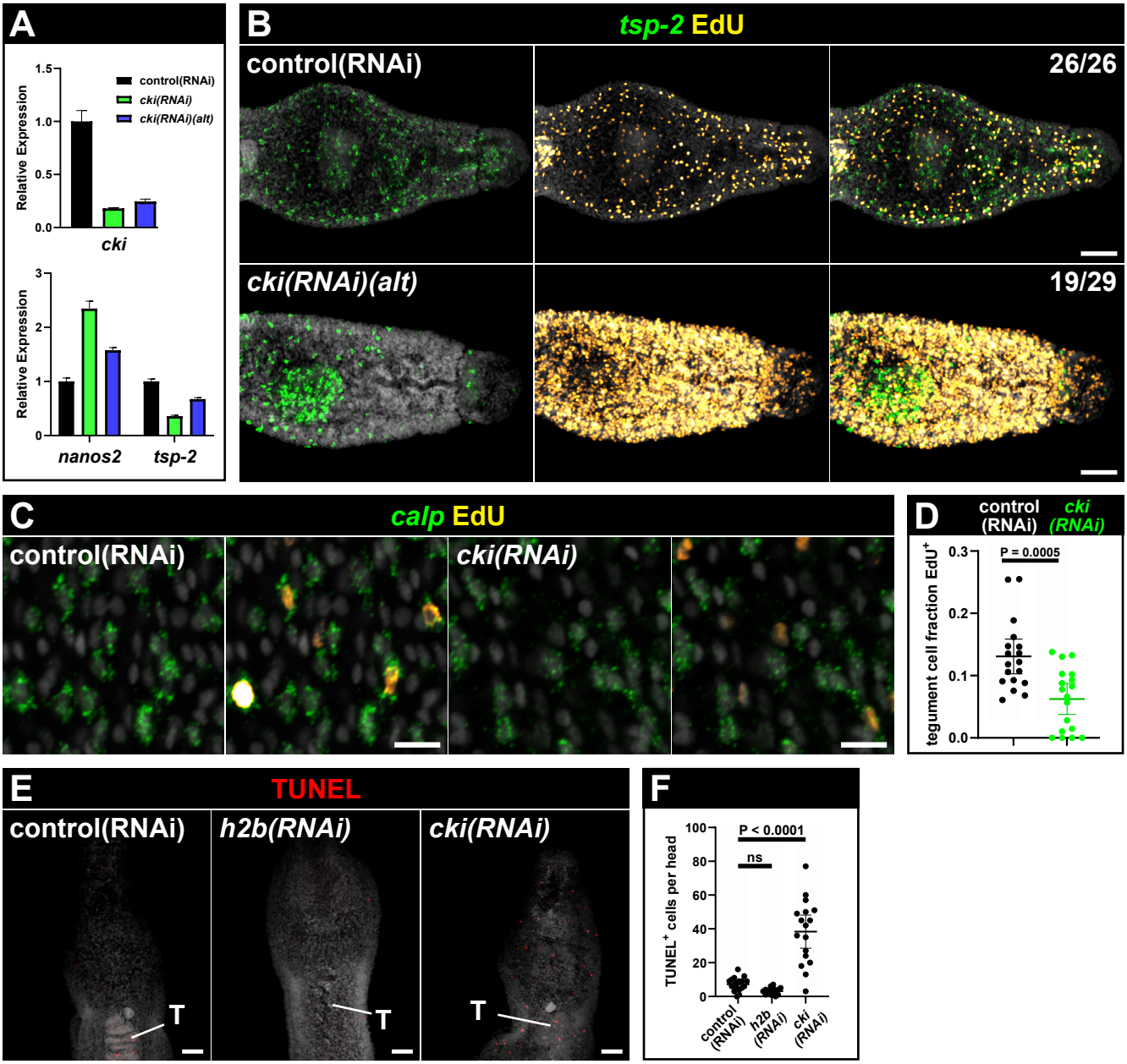

Figure 3: Tumor

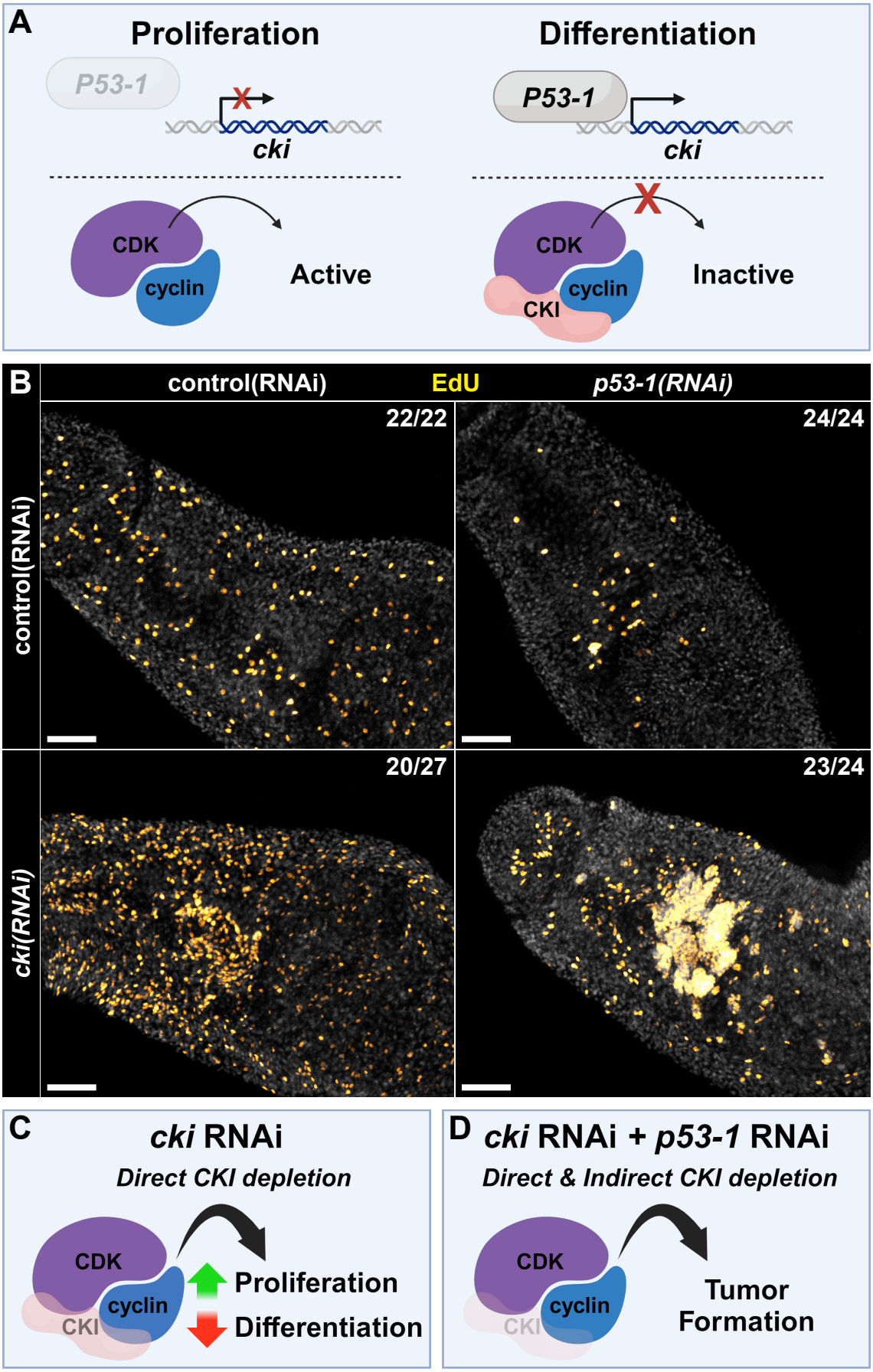

Figure 4: CKI phylogeny

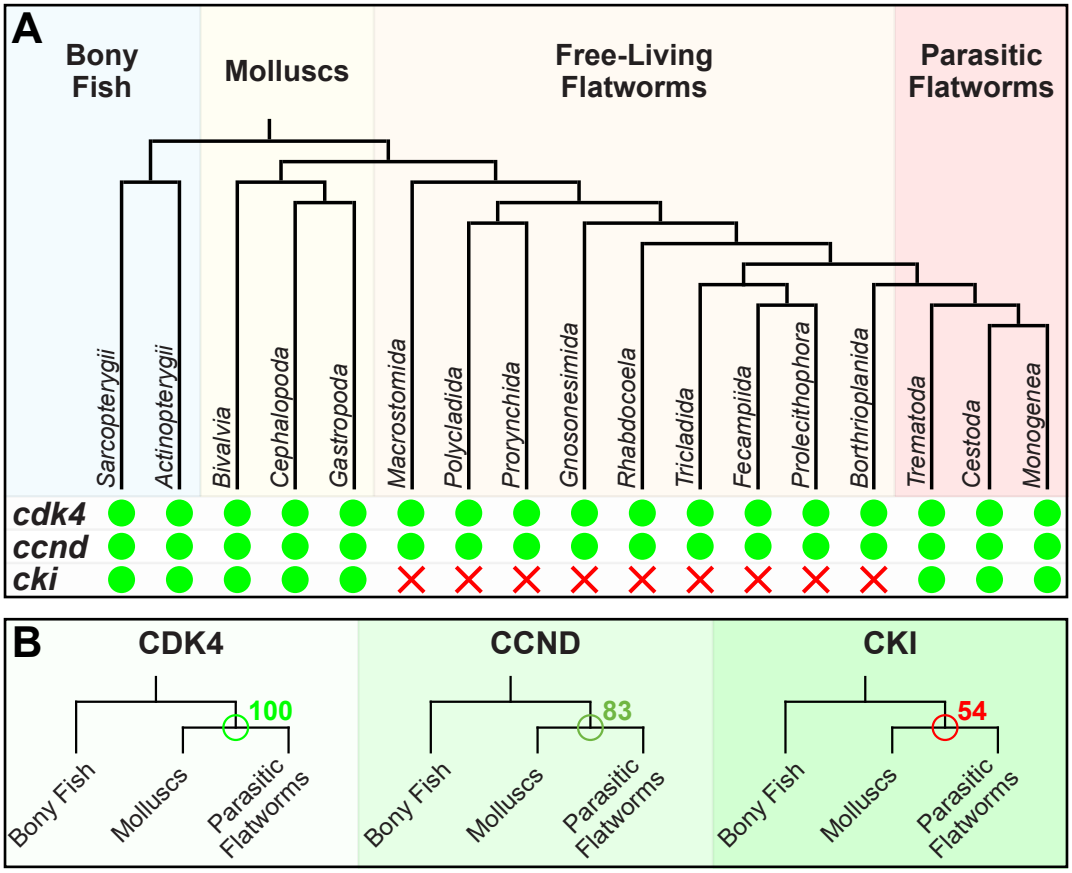

Figure S3: CDK4 phylogeny without free-living flatworms

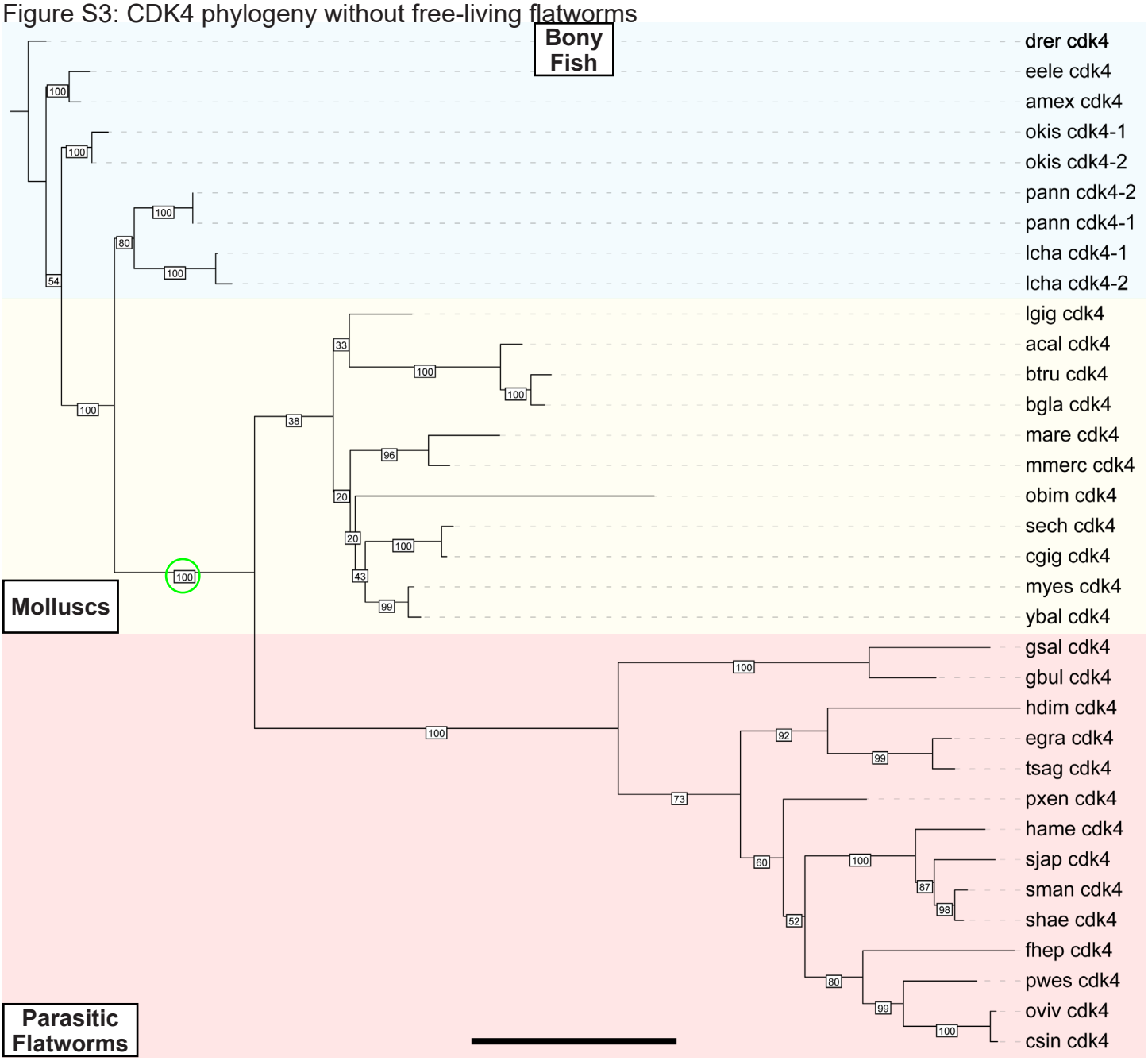

Figure S4: CDK4 phylogeny with free-living flatworms

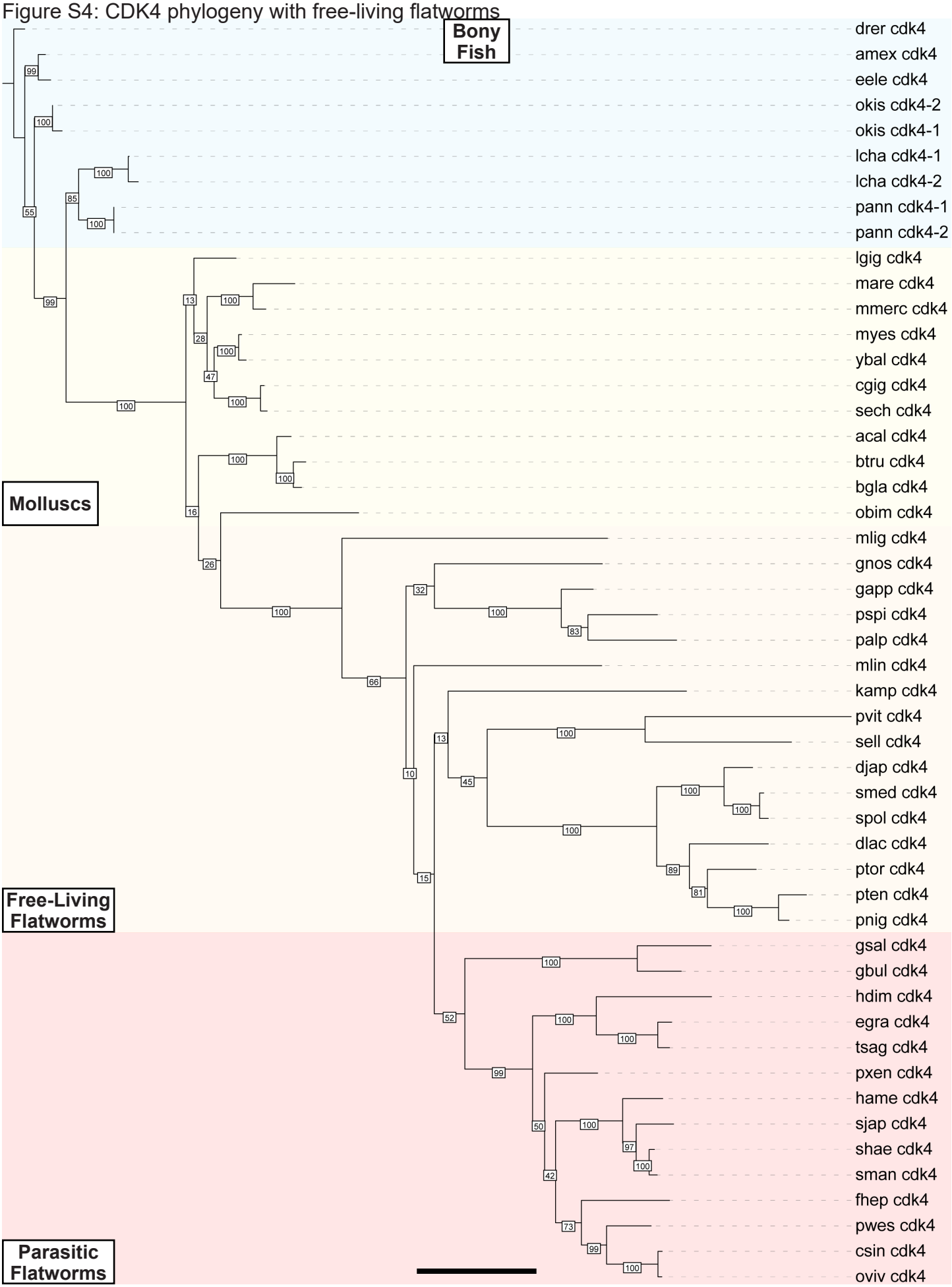

Figure S5: CCND phylogeny without free-living flatworms

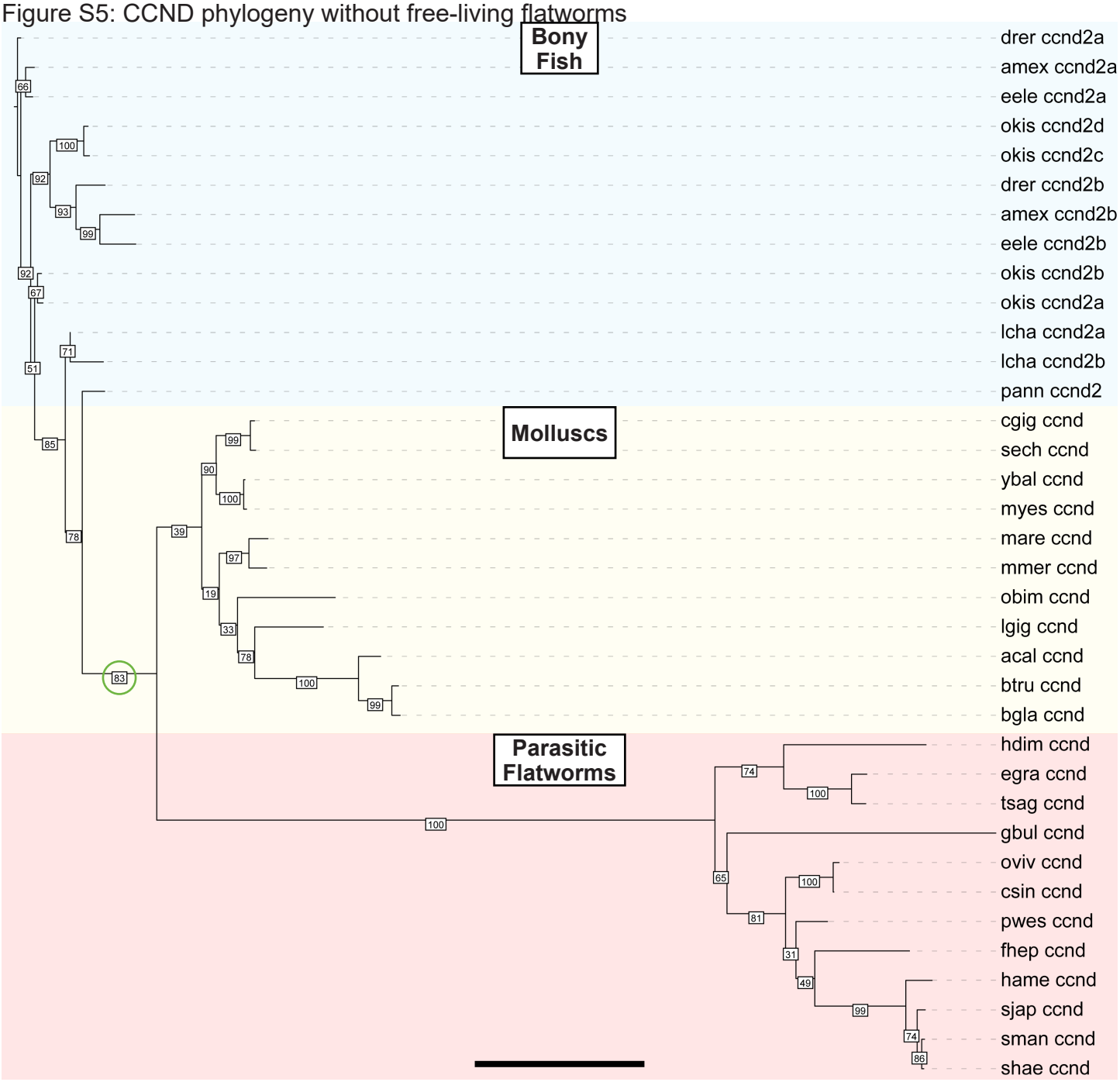

Figure S6: CCND phylogeny with free-living flatworms

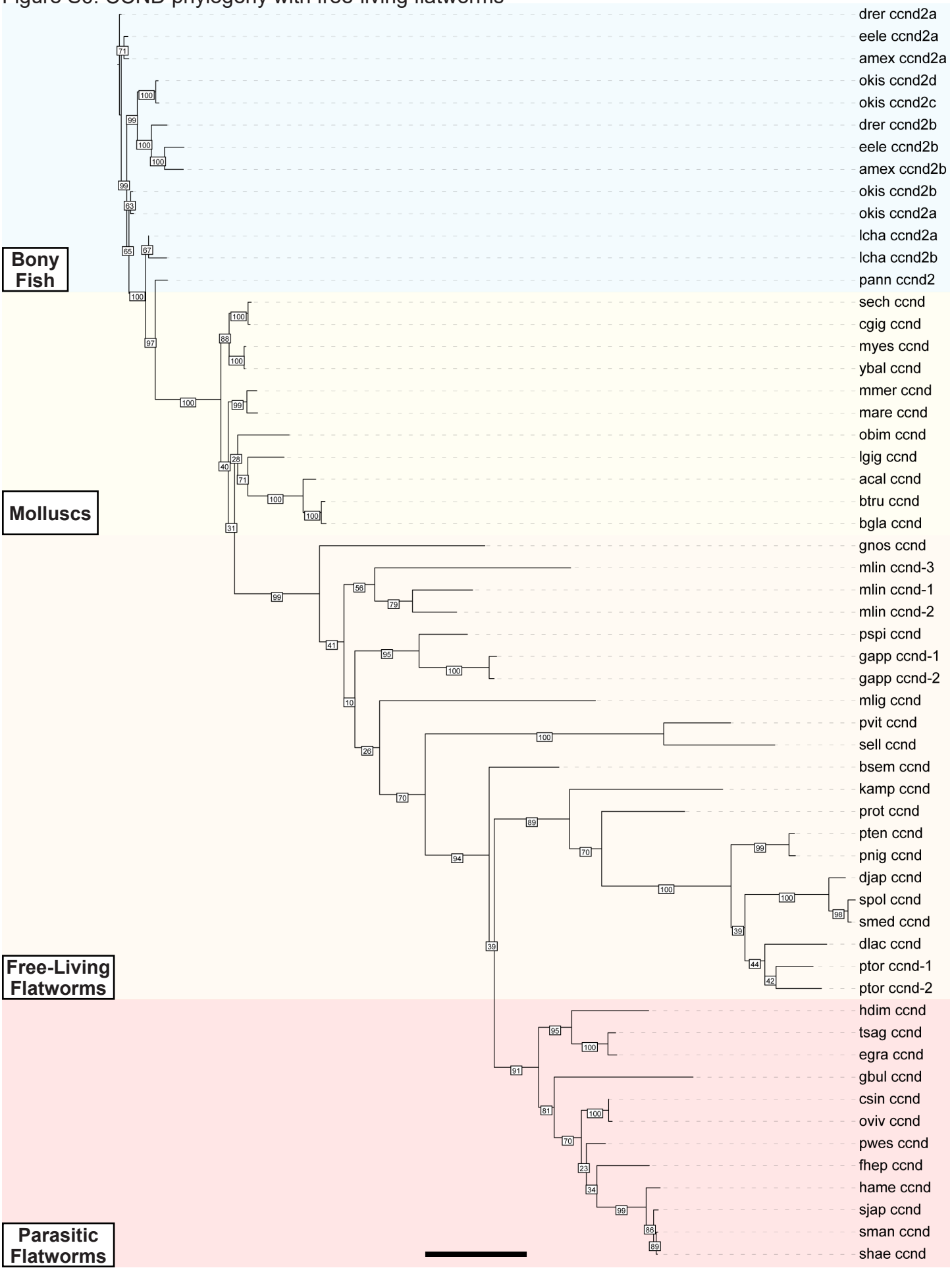
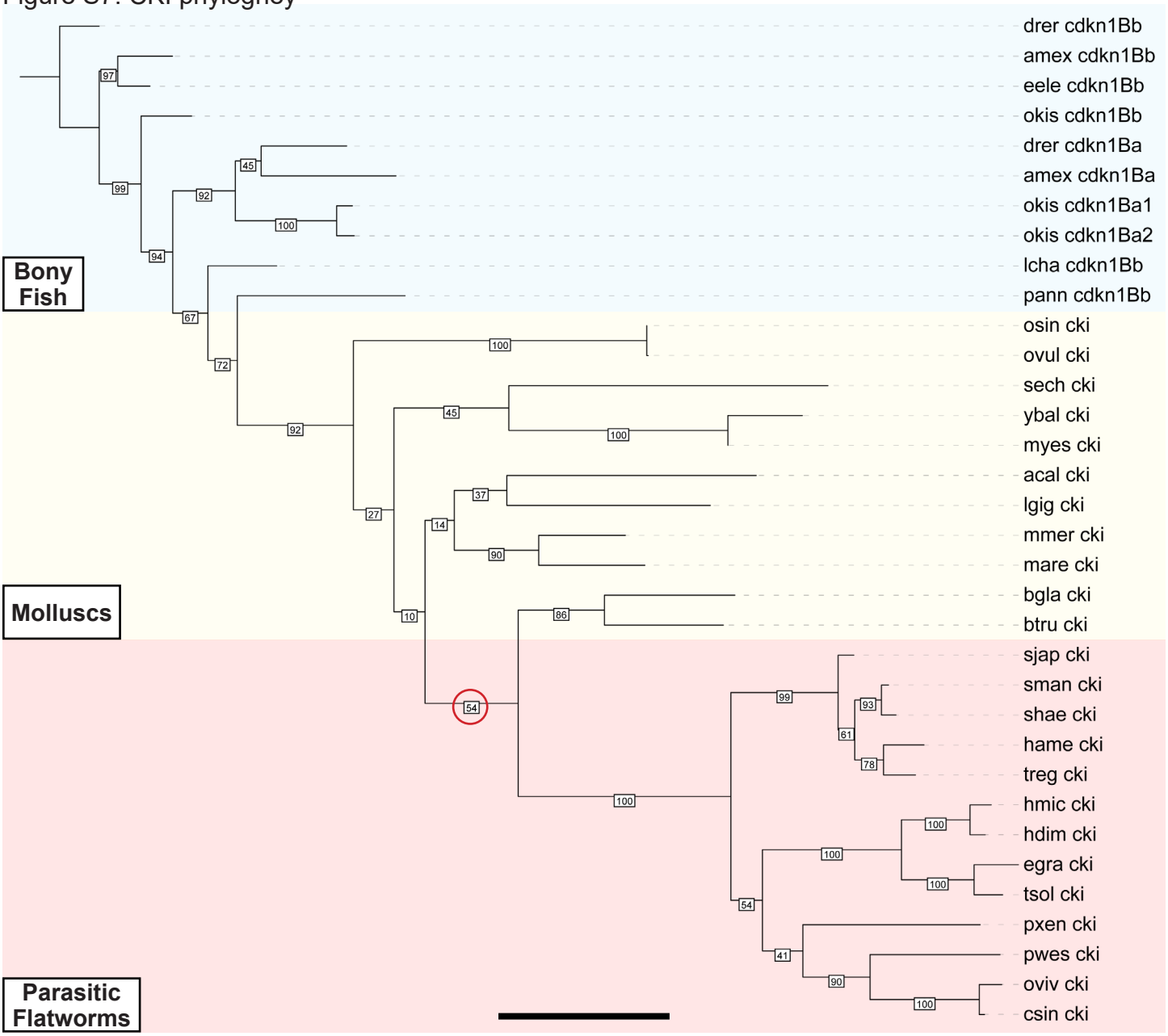
Figure S7: CKI phylogney